

Pulmonary Candidiasis Associated with COVID-19: Evaluation of Causative Agents and their Antifungal Susceptibility Patterns

Fariba Shirvani ¹, Azam Fattahi ²

¹ Pediatric Infections Research Center, Research Institute for Children Health, Shahid Beheshti University of Medical Sciences, Tehran, Iran, ² Center for Research and Training in Skin Diseases and Leprosy, Tehran University of Medical Sciences, Tehran, Iran.

Received: 3 October 2020

Accepted: 26 December 2020

Correspondence to: Fattahi A

Address: Center for Research and Training in Skin Diseases and Leprosy, Tehran University of Medical Sciences, Tehran, Iran

Email address: fattahiazam63@gmail.com

Background: The purpose of the present study was to isolate *Candida* species from individuals with the COVID-19 disease and evaluate the susceptibility pattern of *Candida* spp. to routine antifungal drugs.

Materials and Methods: A total of 25 *Candida* spp. isolated from hospitalized patients with COVID-19, who were suspected to have pulmonary candidiasis, and 26 archived *Candida* spp. specimens were enrolled in this study. For the identification of *Candida* spp., PCR was performed to detect and amplify the ITS1 and ITS4 genes. Then the products were subjected to the Msp I restriction enzyme to precisely identify the species. The amplification of the WHP1 gene was conducted to identify *Candida albicans* species. The antifungal activities of routine drugs and the synthesized AuNPs against *Candida* spp. were assessed based on the protocols presented by the Clinical and Laboratory Standards Institute M60.

Results: In the present study, *C. albicans* (24; 96%) and *C. parapsilosis* (1; 4%) were identified as the etiologic agents of the pulmonary candidiasis associated with the COVID-19 infection. Voriconazol and amphotericin B had superior activity against all the isolates in this study. Treatment with fluconazole and itraconazole did not significantly change the formation of colony-forming units (CFU). However, treatment with the AuNPs significantly decreased (within the range of 92-99.1%; $P < 0.05$) the number of CFUs.

Conclusion: The azole prophylaxis has likely been associated with the development of resistant isolates; the results of the present study suggested the promising role of novel antifungal agents such as AuNPs in overcoming drug resistant fungi.

Key words: Pulmonary candidiasis; COVID 19; Nanoparticles; Azole; Drug resistance

INTRODUCTION

Coronavirus disease 2019 (COVID-19), caused by the severe acute respiratory syndrome coronavirus 2 (SARS-CoV-2), has been an emerging disease and a public health threat worldwide (1). Similar to SARS-CoV and Middle East Respiratory Syndrome Coronavirus (MERS-CoV), COVID-19 causes lower respiratory tract infections and can

lead to Acute Respiratory Distress Syndrome (ARDS) (2). Critically ill individuals, particularly the individuals who are hospitalized in the intensive care unit (ICU) for a long time and require mechanical ventilation, are probable to develop invasive fungal co-infections (3). It is important to consider fungal illnesses in the middle and last stages of COVID-19. Generally, in individuals with severe COVID-

19 who take a broad-spectrum of antibacterial medications, parenteral nutrition, and undergo invasive tests, and in patients with immune deficiency, the risk of candidiasis may be considerably enhanced (3).

Candida spp. are known as opportunistic microorganisms causing severe infections in immunocompromised individuals (4). They can colonize and produce biofilms on every surface, which are extremely resistant to routine antifungals. As resistance to routine antifungal agents is an increasing clinical challenge (5-7), there is a growing need for the development of new and potent antifungals.

Azole antifungals are broadly recommended for the treatment of *Candida* infections. These agents prevent the 14 α -demethylation of lanosterol by blocking cytochrome P450, as an essential enzyme in the ergosterol production pathway (8). A subsequent decrease in ergosterol levels and the accumulation of toxic sterol intermediates in the cytoplasmic membrane lead to growth inhibition (9).

Nanoparticles (NPs) have supposedly higher *in vitro* activities against *C. albicans* than more recently developed and probably more active azoles (10, 11). They are also among valuable options for drug delivery. The combination of NPs with antifungals decreases the risk of toxicity and increases the activities of antifungals (12).

Studying the burden of secondary fungal diseases, their etiologic agents, and the antifungal susceptibility patterns of *Candida* spp. in COVID-19 patients is vital for comprehensively and effectively treating and managing the disease.

The purpose of the present study was to isolate *Candida* species in individuals with COVID-19 and evaluate the susceptibility patterns of *Candida* spp. to routine antifungals. We also assessed the antifungal activities of AuNPs against *C. albicans* and *C. parapsilosis* and checked if these NPs could increase the susceptibility of these fungi to fluconazole and itraconazole.

MATERIALS AND METHODS

Study Areas and Subjects

A total of 25 *Candida* spp. isolated from hospitalized patients with immune suppressive diseases [males: 14 (56%); females: 11 (44%), mean age=60.6 years] and COVID-19, who were suspected to have pulmonary candidiasis and referred to Medical Mycology Laboratory at Research and Training Center for Skin Diseases and Leprosy, Tehran University of Medical Sciences, Tehran, Iran, were enrolled in the current study. Bronchoalveolar lavage (BAL) specimens were collected by bronchoscopy. Furthermore, 26 *Candida* spp. (*C. parapsilosis* [n=25] and *C. albicans* [n=1]) from archived isolates were identified as *Candida* spp. using polymerase chain reaction-restriction fragment length polymorphism. These were isolated from blood cultures and archived specimens in a medical mycology laboratory and used to perform antifungal susceptibility testing against routine antifungals. The efficacy of AuNPs against *C. albicans* and *C. parapsilosis* and their effects in increasing the susceptibility of these fungi to fluconazole and itraconazole were also investigated.

Molecular Identification of Isolates

Extraction of Genomic DNA

Genomic DNA was directly isolated from BAL specimens using a high-pure PCR template purification kit (Roche, Germany) according to the manufacturer's user guide. The extracted DNA was stored at -20°C until further analysis.

Amplification of the ITS Gene

To identify *Candida* spp., PCR was performed to detect the *ITS1* and *ITS4* genes using the following protocol: initial denaturation at 95°C for 10 minutes, 40 cycles of denaturation at 95°C for 20 seconds, annealing at 62°C for 20 seconds, extension at 72°C for 20 seconds, and final extension at 72°C for 5 minutes. Then the products were subjected to the *Msp I* restriction enzyme (Fermentase, USA). The digested fragments were run on a 2% agarose

gel. The amplification of the *WHP1* gene was conducted to identify *C. albicans*, according to a previous report (13).

Synthesis of AuNPs

In order to prepare AuNPs, AuCl₄ (20 mg) (Sigma-Aldrich, St. Louis, MO, USA) was dissolved in 100 µL double-distilled water using a magnetic stirrer. At that point, 150 mg of trisodium citrate (Sigma-Aldrich, St. Louis, MO, USA) was added to the mixture, and then the solution temperature was adjusted to 80 °C. The solution mixture was vigorously stirred in this condition until its color turned to deep red. The solution was cooled down to room temperature. Subsequently, 5 mL of concentrated glycerol was added to the solution under vigorous stirring (14).

Characterization of AuNPs

For the characterization of the sizes and charges of the AuNPs, the Z average size and Zeta potential were estimated using the Malvern Zetasizer Nano ZS90 instrument (Malvern Panalytical Ltd., England).

Antifungal Susceptibility Assay

The minimum inhibitory concentrations (MIC) of fluconazole, itraconazole, voriconazole, amphotericin B, and the synthesized AuNPs were determined according to the Clinical and Laboratory Standards Institute (CLSI) M60 protocol (15). The medium used for these experiments was Roswell Park Memorial Institute 1640 supplemented with L-glutamine, but not sodium bicarbonate (Sigma-Aldrich, St. Louis, MO, USA). The medium also contained 2% w/v glucose (Sigma-Aldrich, St. Louis, MO, USA), and its pH was buffered to 7.0 using MOPS (Sigma-Aldrich, St. Louis, MO, USA). Flat-bottomed 96-well microtiter plates were inoculated with *Candida* spp. to obtain 5×10^5 cells/mL in each well. After 24 h of incubation at 35°C, the absorbance was measured at 590 nm using a microplate reader (Bio-Rad, USA). All the experiments were performed in duplicate. The standard strain of *C. parapsilosis* ATCC 22019 was used as the control in every run. The MIC cut-

off for the antifungals was determined based on the CLSI M60 guideline (15).

Effects of AuNPs on Membrane Permeability in *Candida* spp.

Membrane permeability changes in the *C. albicans* and *C. parapsilosis* exposed to AuNPs were estimated via determining propidium iodide (PI) uptake. Both the treated (i.e., MIC and 2×MIC) and untreated cells were incubated with PI (5 µg/mL) for 15 min. Subsequently, phosphate-buffered saline was used to wash the samples and remove overstraining. Finally, fluorescent images from *C. albicans* and *C. parapsilosis* were recorded using a confocal laser scanning microscope (CLSM; Carl Zeiss, Jena, Germany).

Statistical Analysis

Statistical analysis was performed using SPSS software (version 16.0). The non-parametric Mann-Whitney U test was utilized to compare the results.

RESULTS

According to molecular analyses, only *C. albicans* (24; 96%) and *C. parapsilosis* (1; 4%) (Figure 1A) were identified as the etiologic agents of the pulmonary candidiasis associated with COVID-19. In the present study, no cases of *C. africana* and *C. dubliniensis* were identified based on the amplification of the *HWPI* gene (Figure 1B).

The hydrodynamic sizes of the AuNPs ranged from 7 to 15 nm, and the polydispersity index (PI) was reported as 0.395 (Figure 2). The zeta potential of the AuNPs was obtained as -22.4 mV (Figure 3).

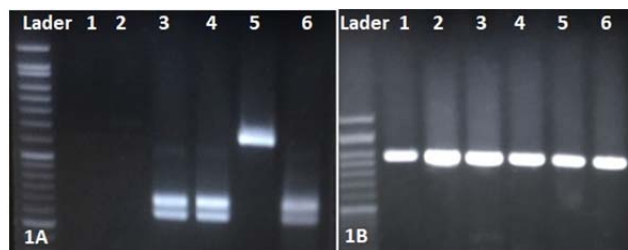


Figure 1. A) PCR-RFLP gel electrophoresis pattern using the *MspI* restriction enzyme: lader: marker 100 bp; lan 1,2 negative control, lan 3,4,6 *C. albicans* (238-297 bp), lan 5 *C. parapsilosis* (500 bp). B) Agarose gel of PCR amplification with *HWPI* gene;1-6 *C. albicans* ~ 900 bp.

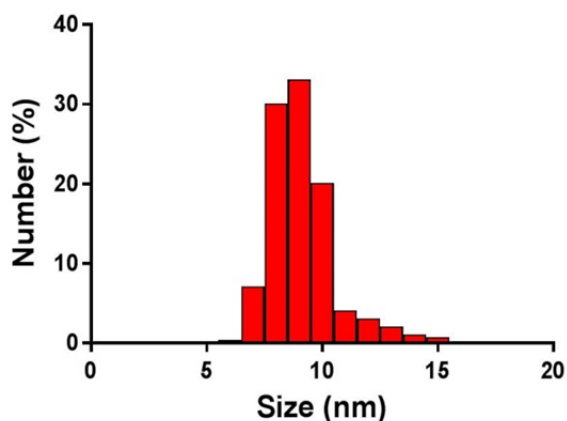


Figure 2. Dynamic light scattering profile of gold nanoparticles indicating effective size of 9 nm (size range: 7-15 nm) and polydispersity index of 0.395

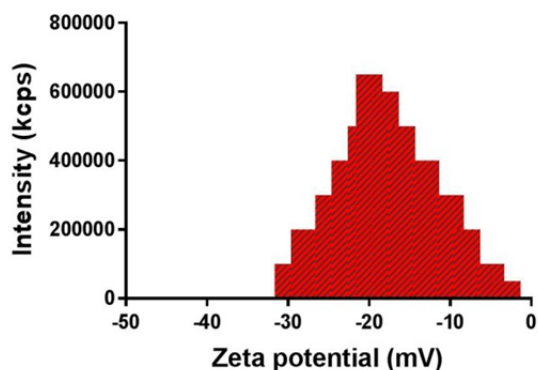


Figure 3. Zeta potential profile of gold nanoparticles

Table 1 describes the MICs and MICs 90 of all the antifungals assessed. Voriconazol and amphotericin B had superior activity against all the evaluated isolates. The MICs of fluconazole and itraconazole varied for the tested isolates. For three *C. albicans* clinical isolates from the present study, the MICs of fluconazole and itraconazole were ≥ 32 and 16 $\mu\text{g/mL}$, respectively. In the case of *C.*

parapsilosis, the MICs of four clinical isolates (one from the present study) were 64 and $\geq 8 \mu\text{g/mL}$ for fluconazole and itraconazole, respectively.

All other isolates showed sensitivity to all the antifungal compounds used in the present study.

The MIC of AuNPs was lower than those reported for fluconazole and itraconazole ($P < 0.05$). The effect of the AuNPs on fluconazole- and itraconazole-resistant *Candida* spp. was determined (Figure 4). While treatment with fluconazole and itraconazole did not lead to a significant change in the formation of colony-forming units (CFU), treatment with the AuNPs significantly decreased (range: 92-99.1%; $P < 0.05$) the number of CFUs. The lowest decrease (92%) was related to *C. parapsilosis* (no. 34), and the highest reductions (99.1%) were recorded for *C. albicans* (no. 1) and *C. parapsilosis* (no. 11). These findings indicated the fungicidal properties of the synthesized AuNPs against *Candida* cells.

The effects of the produced AuNPs on the viability of *C. albicans* and *C. parapsilosis* were studied using CLSM and PI staining. Figure 5 depicts the CLSM images of stained cells of *C. albicans* and *C. parapsilosis* before and after treatment with AuNPs. The uptake of PI by *C. albicans* and *C. parapsilosis* showed concentration-dependent mortality following treatment with the AuNPs. No or rare PI-stained cells were observed in the control group (Figure 5A), indicating an intact cell wall structure of *C. glabrata*. However, a substantial number of PI-stained cells exhibited red fluorescence in the groups treated with the AuNPs (Figure 5).

Table 1. MICs range and MICs 90 of four antifungals were computed for *Candida* species

Fungi Species		Amphotericin B	Voriconazole	Itraconazole	Fluconazole
		$\mu\text{g/mL}$	$\mu\text{g/mL}$	$\mu\text{g/mL}$	$\mu\text{g/mL}$
<i>Candida</i>	MICs Range MIC90	0.003-0.5	0.003-1	0.003-16	0.12564
		0.003	0.003	0.5	0.5

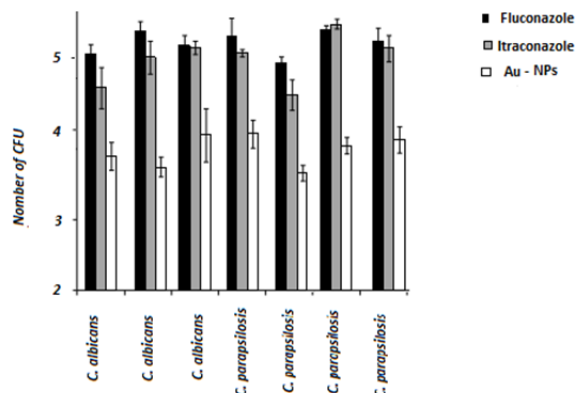


Figure 4. Number of colony-forming units (logarithmic) per minimum inhibitory concentration of *Candida* cells in the presence of antifungals; black bars: cells treated with fluconazole; grey bars: cells treated with itraconazole; white bars: cells treated with gold nanoparticles; statistical analysis using Mann-Whitney U test showing significant differences in cells biomass between azole-treated and nanoliposome-treated for all tested strains ($P < 0.05$), but not between fluconazole-treated and itraconazole-treated cells

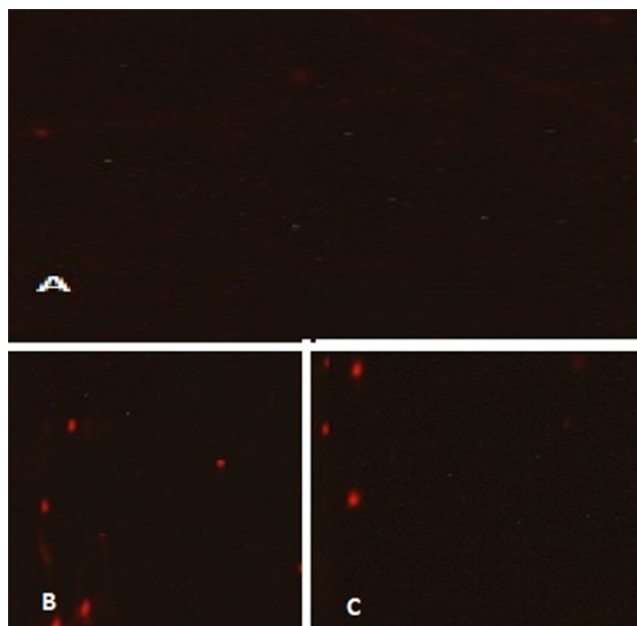


Figure 5. Confocal laser scanning microscopy images of propidium iodide stained. (A) control; (B) *C. albicans*, and (C) *C. parapsilosis* treated with 0.5 µg/ml of gold nanoparticles

DISCUSSION

There is limited information about the burden of candidiasis in critically ill COVID-19 patients. In the present study, *C. albicans* (24; 96%) and *C. parapsilosis* (1;

4%) were identified as the most common etiologic agents of the pulmonary candidiasis associated with the COVID-19 infection. Consistently, a study in Spain reported candidemia, candiduria, and complicated intraabdominal candidiasis among COVID-19 patients (16). A study in the UK reported a prevalence of 14.1% for invasive candidiasis among the COVID-19 patients who had ARDS (17). Three candidemia cases were reported in the critically ill COVID-19 patients treated with tocilizumab, an IL-6 inhibitor (18). In other studies, infections due to *C. albicans*, *C. auris*, *C. glabrata*, *C. parapsilosis*, *C. tropicalis*, and *C. krusei* were reported to be common among critically ill COVID-19 patients (17-23).

Similar to other studies, the drug resistance patterns of fungi in our study varied depending on the species. In previous reports, resistance to fluconazole, multiple azoles (fluconazole and voriconazole), and multidrug regimens (fluconazole and AMB) was noted for 100%, 30%, and 40% of *C. auris* isolates, respectively, and only one *C. glabrata* isolate was echinocandin-resistant (17-23).

The present study was conducted to determine if AuNPs could directly or indirectly affect the structure of the cytoplasmic membrane of azole-resistant *Candida* spp., resulting in the altered viability of these cells (Figure 5). The membrane's morphology on microscopic examination differed comparing untreated non-WT cells and AuNPs-treated mutant cells. The cytoplasmic membranes of the resistant strains were disrupted after exposure to AuNPs.

As the *Candida* spp. selected in the current study can cause severe invasive candidiasis, the favorable broad-spectrum fungicidal activity of the synthesized AuNPs can be of critical importance for treating the drug-resistant fungi causing pulmonary candidiasis in COVID-19 patients.

The *in vitro* concentrations of the produced AuNPs used in the present study may be never applicable *in vivo* to manage and treat invasive candidiasis caused by drug-resistant fungi. For instance, most cases of candidemia are caused by *Candida* spp. colonization and biofilm production on medical devices (24). It seems that the

AuNP concentrations applied here can prevent biofilm formation on medical devices.

A recently developed delivery system for antifungals can be used to enhance the fungicidal properties of AuNPs (25, 26). The findings of the present study raised the hypothesis that the fungicidal activity of azoles against resistant fungi can be enhanced in conjugation with AuNPs. The results of the current study suggested that the incorporation of AuNPs with candidate azoles at the N1-4 position could promote a synergistic effect.

CONCLUSION

Efforts have been made to develop new antifungal agents or boost the efficiency of the present ones for treating severe pulmonary candidiasis in COVID-19 patients. Although azole prophylaxis has likely been associated with the development of resistant isolates, the results of the present study suggested the promising role of novel antifungal agents such as AuNPs in overcoming drug resistant fungi.

REFERENCES

- Zu ZY, Jiang MD, Xu PP, Chen W, Ni QQ, Lu GM, et al. Coronavirus Disease 2019 (COVID-19): A Perspective from China. *Radiology* 2020;296(2):E15-E25.
- Mohanty SK, Satapathy A, Naidu MM, Mukhopadhyay S, Sharma S, Barton LM, et al. Severe acute respiratory syndrome coronavirus-2 (SARS-CoV-2) and coronavirus disease 19 (COVID-19) - anatomic pathology perspective on current knowledge. *Diagn Pathol* 2020;15(1):103.
- Arastehfar A, Carvalho A, Nguyen MH, Hedayati MT, Netea MG, Perlin DS, et al. COVID-19-Associated Candidiasis (CAC): An Underestimated Complication in the Absence of Immunological Predispositions? *J Fungi (Basel)* 2020;6(4):211.
- Leite MC, Bezerra AP, de Sousa JP, Guerra FQ, Lima Ede O. Evaluation of Antifungal Activity and Mechanism of Action of Citral against *Candida albicans*. *Evid Based Complement Alternat Med* 2014;2014:378280.
- Alves IA, Bandeira LA, Mario DA, Denardi LB, Neves LV, Santurio JM, et al. Effects of antifungal agents alone and in combination against *Candida glabrata* strains susceptible or resistant to fluconazole. *Mycopathologia* 2012;174(3):215-21.
- Lee JH, Kim YG, Gupta VK, Manoharan RK, Lee J. Suppression of Fluconazole Resistant *Candida albicans* Biofilm Formation and Filamentation by Methylindole Derivatives. *Front Microbiol* 2018;9:2641.
- Thomaz DY, de Almeida JN Jr, Lima GME, Nunes MO, Camargo CH, Grenfell RC, et al. An Azole-Resistant *Candida parapsilosis* Outbreak: Clonal Persistence in the Intensive Care Unit of a Brazilian Teaching Hospital. *Front Microbiol* 2018;9:2997.
- Yoshida Y. Cytochrome P450 of fungi: primary target for azole antifungal agents. *Curr Top Med Mycol* 1988;2:388-418.
- Nett JE, Andes DR. Antifungals: Drug Class, Mechanisms of Action, Pharmacokinetics/Pharmacodynamics, Drug-Drug Interactions, Toxicity, and Clinical Use. *Candida and candidiasis* 2011:343-71.
- Stoimenov PK, Klinger RL, Marchin GL, Klabunde KJ. Metal oxide nanoparticles as bactericidal agents. *Langmuir* 2002;18(17):6679-86.
- Jebali A, Hajjar FH, Pourdaneh F, Hekmatimoghaddam S, Kazemi B, Masoudi A, et al. Silver and gold nanostructures: antifungal property of different shapes of these nanostructures on *Candida* species. *Med Mycol* 2014;52(1):65-72.
- Chen M, Yang Z, Wu H, Pan X, Xie X, Wu C. Antimicrobial activity and the mechanism of silver nanoparticle thermosensitive gel. *Int J Nanomedicine* 2011;6:2873-7.
- Fattahi A, Lotfali E, Masoumi-Asl H, Sayyahfar S, Kalani M, Rafi Khourgami M, et al. Candidemia and its Risk Factors in Neonates and Children. *Archives of Pediatric Infectious Diseases* 2020;8(4): e101431.
- Tabrizi A, Ayhan F, Ayhan H. Gold nanoparticle synthesis and characterisation. *Hacettepe Journal of Biology And Chemistry* 2009;37(3):217-26.
- Institute CLS. Reference Method for Broth Dilution Antifungal Susceptibility Testing of Yeasts. CLSI standard M60. Clinical and Laboratory Standards Institute Wayne, PA; 2017.
- Garcia-Vidal C, Sanjuan G, Moreno-García E, Puerta-Alcalde P, Garcia-Pouton N, Chumbita M, et al. Incidence of co-

- infections and superinfections in hospitalized patients with COVID-19: a retrospective cohort study. *Clin Microbiol Infect* 2021;27(1):83-8.
17. White PL, Dhillon R, Cordey A, Hughes H, Faggian F, Soni S, et al. A national strategy to diagnose COVID-19 associated invasive fungal disease in the ICU. *Clin Infect Dis* 2020:ciaa1298.
 18. Antinori S, Bonazzetti C, Gubertini G, Capetti A, Pagani C, Morena V, et al. Tocilizumab for cytokine storm syndrome in COVID-19 pneumonia: an increased risk for candidemia? *Autoimmun Rev* 2020;19(7):102564.
 19. Ventoulis I, Sarmourli T, Amoiridou P, Mantzana P, Exindari M, Gioula G, et al. Bloodstream Infection by *Saccharomyces cerevisiae* in Two COVID-19 Patients after Receiving Supplementation of *Saccharomyces* in the ICU. *J Fungi (Basel)* 2020;6(3):98.
 20. Salehi M, Ahmadikia K, Mahmoudi S, Kalantari S, Jamalimoghadamsiahkali S, Izadi A, et al. Oropharyngeal candidiasis in hospitalised COVID-19 patients from Iran: Species identification and antifungal susceptibility pattern. *Mycoses* 2020;63(8):771-8.
 21. Posteraro B, Torelli R, Vella A, Leone PM, De Angelis G, De Carolis E, et al. Pan-Echinocandin-Resistant *Candida glabrata* Bloodstream Infection Complicating COVID-19: A Fatal Case Report. *J Fungi (Basel)* 2020;6(3):163.
 22. Al-Hatmi AMS, Mohsin J, Al-Huraizi A, Khamis F. COVID-19 associated invasive candidiasis. *J Infect* 2021;82(2):e45-e46.
 23. Chowdhary A, Tarai B, Singh A, Sharma A. Multidrug-Resistant *Candida auris* Infections in Critically Ill Coronavirus Disease Patients, India, April-July 2020. *Emerg Infect Dis* 2020;26(11):2694-96.
 24. Kojic EM, Darouiche RO. *Candida* infections of medical devices. *Clin Microbiol Rev* 2004;17(2):255-67.
 25. Wani IA, Ahmad T, Manzoor N. Size and shape dependant antifungal activity of gold nanoparticles: a case study of *Candida*. *Colloids Surf B Biointerfaces* 2013;101:162-70.
 26. Rahimi H, Roudbarmohammadi S, Delavari H H, Roudbary M. Antifungal effects of indolicidin-conjugated gold nanoparticles against fluconazole-resistant strains of *Candida albicans* isolated from patients with burn infection. *Int J Nanomedicine* 2019;14:5323-38.